Solar Energy Materials & Solar Cells 129 (2014) 90–94

Contents lists available at ScienceDirect

Solar Energy Materials & Solar Cells

journal homepage: www.elsevier.com/locate/solmat

Increased performance of inverted organic photovoltaic cells using a cationically functionalized fullerene interfacial layer

Christopher D. Weber, Colin Bradley, Ethan M. Walker, Stephen G. Robinson, Mark C. Lonergan *

Department of Chemistry, University of Oregon, Eugene, OR 97403, USA

ARTICLE INFO

Available online 6 April 2014

Keywords:
Organic photovoltaic
Inverted structure
Interfacial layer
Cationically functionalized
Fullerene

ABSTRACT

The incorporation of a cationically functionalized fullerene interfacial layer (NMFP-Br) into an inverted poly(3-hexylthiophene):[6,6]-phenyl-C_{61}-butyric acid methyl ester (P3HT:PCBM) bulk heterojunction photovoltaic cell results in a significant power conversion efficiency (PCE) improvement of 67%, from 2.1% to 3.5%, relative to cells without an interfacial layer. The incorporation of NMFP-Br as an ITO modifying interfacial layer results in a 190 mV increase in the open-circuit voltage, 13% increase in fill factor, and 250% reduction in series resistance. Cell efficiencies are greater than or comparable to other reported cells based on organic electron injection layers with the same active layer and electrode configuration. The orthogonal solubility afforded by ionic functionality allows for sequential solution phase deposition without the necessity of chemical cross-linking of the fullerene based interfacial layer. Inverted devices incorporating a single phase, ionically functionalized fullerene interfacial layer have not been previously demonstrated. The unusually high conductivity of NMFP-Br films is investigated and shown to be ~3 orders of magnitude higher than PCBM and contributes to the substantial reduction in series resistance.

1. Introduction

Electrode modification using interfacial layers (IFLs) to enhance the performance of inverted organic photovoltaic cells (i-OPVs) has attracted increased research interest in recent years [1–3]. Modification of electrodes using IFLs has been shown to have a significant impact on the magnitude of the cell's open-circuit voltage (V_{oc}) [2–4]. This enhancement of V_{oc} can result from the modification of the electrode work function to increase the built-in potential, as well as enhanced alignment of the electrode work function with the active layer quasi Fermi level for electrons or holes. IFL modification of electrodes can also provide charge selectivity by introducing an energy barrier to a specific sign of charge. This charge selectivity reduces interfacial recombination at the collecting electrode resulting in an increase in V_{oc} [5]. To maximize performance of devices, it is also important to ensure a low series resistance (R_s) to maximize charge extraction and enhance the fill factor (FF) [6].

Numerous IFLs have been investigated to modify the transparent electron-collecting electrode, typically indium tin oxide (ITO), in i-OPVs. These include n-type wide bandgap semiconductors such as TiO_2 [7] and ZnO [8], graphene [9], fullerene films [10,11] and self-assembled monolayers (SAMs) [12,13], conjugated polymers [1], and conjugated polyelectrolytes (CPEs) [14]. The use of ion-containing IFL materials, such as CPEs, are particularly attractive as they posses orthogonal solubility to most active layer bulk heterojunction (BHJ) blends which facilitates solution processability. Furthermore, CPEs containing cationic functional groups have been shown to effectively reduce the ITO work function, which defines the ITO polarity and promotes Fermi level alignment with the acceptor phase in the inverted structure [15–17].

Fullerene based IFLs have recently gained interest as efficient electron collecting electrode interfacial layers (n-IFLs) in inverted and conventional BHJ solar cells. Fullerene derivatives are advantageous as n-IFLs due to their energy-level alignment with the PCBM acceptor phase, resulting in efficient charge transfer with minimal voltage loss. In addition, the low-lying HOMO level of fullerenes enhances carrier selectivity by inhibiting hole transfer from the donor polymer. Cationically functionalized fullerene n-IFLs have been demonstrated by Jen et al. in conventional OPVs [18]; however, due to poor solvent resistance, fullerene n-IFLs in the inverted geometry have often required chemical cross-linking or the use of fullerene SAMs which are chemically bound to the substrate [19,20]. The relatively low conductivity of fullerene n-IFLs has also often required the use of an underlying n-type IFL such as TiO_2 to reduce R_s [2,12]. To overcome this shortcoming,

* Corresponding author. Tel.: +1 54 134 647 48.
E-mail address: lonergan@uoregon.edu (M.C. Lonergan).

http://dx.doi.org/10.1016/j.solmat.2014.03.034
0927-0248/

chemical n-doping of fullerene IFLs by co-evaporation with Cs_2Co_3 or incorporation of n-dopants, such as decamethylcobaltacene or alkali carbonates have been reported [10,20,21].

Herein we demonstrate the use of the highly conductive, alcohol-soluble, cationically functionalized fullerene derivative N,N,N-trimethyl-5-(N-methyl-3,4-[60]fulleropyrrolidin-2-yl)pentan-1-aminium bromide (NMFP-Br) as an efficient electron collecting electrode interfacial layer in poly(3-hexylthiophene):[6,6]-phenyl-C_{61}-butyric acid methyl ester (P3HT:PCBM) inverted organic photovoltaic cells. The incorporation of NMFP-Br as an n-IFL results in a substantial increase of the V_{oc} from 0.41 V to 0.60 V and the overall power conversion efficiency (PCE) from 2.1% to 3.5% under AM 1.5G illumination. The orthogonal solubility of NMFP-Br allows for sequential solution processing without the need of chemical cross-linking. The unusually high conductivity of this material results in a significant decrease in the series resistance, relative to control devices, even when the n-IFL thickness is increased fivefold.

2. Experimental

2.1. Synthesis of N,N,N-trimethyl-5-(N-methyl-3,4-[60] fulleropyrrolidin-2-yl)pentan-1-aminium bromide (NMFP-Br)

Sarcosine (0.3 g, 3.4 mmol) and 6-bromo-hexanal (240 mg, l.34 mmol) were added to a solution of C_{60} (654 mg, 0.91 mmol) in deoxygenated toluene (600 mL). The solution was heated to a reflux for 2 h turning from purple to a dark brown at which point it was cooled to room temperature, concentrated to ~100 mL and then purified by silica gel column chromatography using toluene as eluent. Eluting first was unreacted purple starting material, followed by the mono-adduct (300 mg) followed by multiple addition products (240 mg). Trimethylamine (3 mL) was added to a solution of the mono adduct (170 mg, 0.18 mmol) in $CHCl_3$ (200 mL) at 0 °C, the flask was sealed and the solution was allowed to warm to room temperature. After stirring for 5 days, N_2 was bubbled through the solution for 1 h with the gas afterwards being passed through an HCl column (removes the NMe_3 as the hydrochloride salt). The solvent was evaporated and the solid was washed with a small amount of methanol to give the product as a brown powder (142 mg, 0.14 mmol, 78%).

^{1}H NMR (600 MHz, $CDCl_3$) δ 4.82 (*d*, 1H, J=9.7 Hz), 4.17 (*d*, IH, J=9.6 Hz), 3.91 (*t*, 1H, J=5.3 Hz), 3.43 (*t*, 2H, J=6.5 Hz), 2.99 (*s*, 3H), 2.57–2.52 (*m*, 1H), 2.43–2.38 (*m*, 1H), 2.0–1.91 (*m*, 4H), 1.64 (quin, 2H, J=7.5 Hz)

^{13}C NMR (151 MHz, $CDCl_3$) δ 156.60, 154.64, 154.47, 153.47, 147.44, 147.40, 146.86, 146.58, 146.52, 146.49, 146.45, 146.37, 146.35, 146.29, 146.24, 146.17, 146.14, 145.98, 145.75, 145.65, 145.61, 145.58, 145.54, 145.50, 145.48, 145.42, 145.38, 144.93, 144.76, 144.61, 144.54, 143.38, 143.26, 143.34, 142.89, 142.85, 142.82, 142.80, 142.39, 142.35, 142.33, 142.27, 142.25, 142.23, 142.03, 141.92, 141.88, 140.47, 140.39, 139.98, 139.85, 137.38, 136.39, 136.05, 135.66, 129.19, 128.38, 78.20, 76.40, 70.60, 70.31, 40.21, 33.87, 32.65, 31.04, 28.94, 26.72.

2.2. Device fabrication

Inverted devices were fabricated using patterned ITO coated slides (R_s~5–15 Ω/□) sequentially cleaned with detergent solution (Micro-90), acetone, and isopropyl alcohol in a sonicator for 15 min each. NMFP-Br was spin cast from dilute methanol solution (< 0.5 mg/mL) or DMSO:1% H_2O (5 mg/mL) solution at 1000 and 500 rpm for 60 s and 16 min respectively. Devices were annealed in vacuo for 90 min at 110 °C. NMFP-Br coated and control substrates were transferred to a nitrogen filled glovebox for further fabrication. An active layer blend (1:0.8 wt%/conc. 43 mg/mL) of P3HT (Sigma Aldrich) and PCBM (SRS Research) was prepared in deoxygenated ortho-dichlorobenzene (Sigma Aldrich). The active layer was spin cast at 900 rpm for 20 s and allowed to slow dry for 10 min followed by annealing at 110 °C for 5 min resulting in an active layer thickness of 160 nm. PEDOT:PSS (Sigma Aldrich) was then spin cast from a 1:5 dilution in isopropyl alcohol at 4000 rpm for 60 s followed by a 10 min anneal at 120 °C. A second PEDOT:PSS layer was then applied and annealed following the same parameters. Gold (45 nm) was deposited at a pressure $< 10^{-6}$ m Torr through a shadow mask to define a device area of 0.03 cm^2 (device architecture shown in Fig. 1a). No significant differences in device properties were observed using thicker gold contacts.

2.3. Measurements

Device layer thicknesses were determined using a Dektak stylus profilometer. Current density–voltage (J–V) measurements were taken using a Keithley 2400 or 236 source measure unit. Photocurrent density–voltage measurements were performed using an AM 1.5G solar simulator (Oriel) calibrated to 97 mW/cm^2 with a thermopile power meter. External quantum efficiencies (EQE) were determined using a custom designed spectrometer and an Agilent 4156C source measure unit. UV–vis–NIR measurements were performed under airfree conditions using a Perkin-Elmer series 1050 spectrometer.

3. Results and discussion

The average J–V curves of inverted devices with and without NMFP-Br n-IFLs are shown in Fig. 2 and properties are tabulated in Table 1. The J–V curves initially display an S-shaped kink which is often observed in inverted devices incorporating metal oxide or CPE interlayers [17,30]. In the case of inverted cells incorporating a

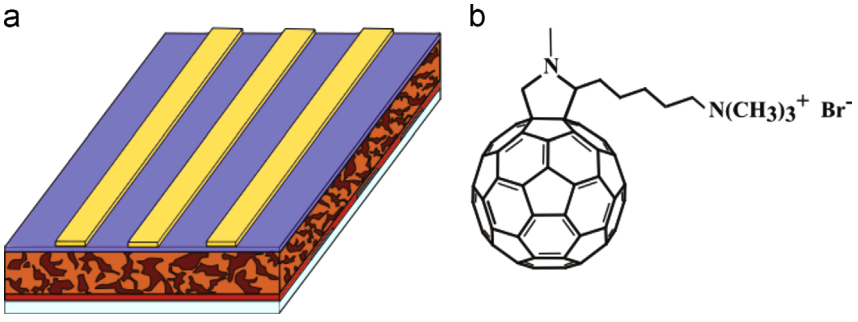

Fig. 1. (a)Architecture of inverted device: glass substrate/ITO/NMFP-Br/P3HT:PCBM/PEDOT:PSS/Au with an ITO and Au electrode overlap area of 0.03 cm^2 and (b) the chemical structure of NMFP-Br.